SUPPLEMENTARY MATERIAL

Galectin-1 drives pancreatic carcinogenesis through stroma remodeling and Hedgehog signaling activation

Neus Martínez-Bosch[1], Maite G. Fernández-Barrena[2], Mireia Moreno[1], Elena Ortiz-Zapater[1‡], Sabine André[3], Hans-Joachim Gabius[3], Rosa F. Hwang[4], Françoise Poirier[5], Jessica Munné-Collado[1,6], Mar Iglesias[1,6], Carolina Navas[7], Carmen Guerra[7], Martin E. Fernández-Zapico[2], and Pilar Navarro[1]

Content:

Supplementary Text

Ela-myc Gal1 macroscopic tumor characterization

Ela-myc:Gal1$^{+/+}$, *Ela-myc:Gal1*$^{+/-}$ and *Ela-my:Gal1*$^{-/-}$ mice were sacrificed when they displayed signs of advanced disease (ages oscillate between 1.8 and 7.3 months), and tumors were collected and analyzed. All three genotypes displayed irregularly shaped tumors, with 1.5-2 cm in diameter, occupying almost the whole pancreas; normal pancreas was rarely found and frequently atrophic. At the macroscopic level, tumors were either soft and red – with hemorrhagic cysts–, or yellowish and with solid appearance. In general, one large or several smaller tumoral nodules were found, with frequent infiltration of peripancreatic lymph nodes. Although a tendency to exert less lymph node infiltration in tumors from heterozygous or null Gal1 mice was seen (27.3% and 27.9% respectively, in comparison to 31.8% in the *Ela-myc* wt mice), data did not reach statistical significance (Supplementary Table 1). Occasionally, macroscopic tumoral foci were also detected in diaphragm, kidney, liver, intestine, stomach and spleen but no significant correlation between genotype and metastasis frequency was observed (Supplementary Table 1).

Gal1 downregulation in pancreatic cancer cells is not sufficient to impair tumor progression in xenografts

To address the specific contribution of Gal1 expressed by pancreatic cancer epithelial cells to *in vivo* tumor progression, luciferase expressing PANC-1 cells (PANC-1LUC) untransfected (wt), transfected with shCtl or with shGal1#1 and shGal1#2, were intraperitoneally injected into nude mice and their tumorigenic

properties analyzed. Most of the animals developed tumors in the pancreas with histopathological hallmarks of PDA (Supplementary Figure S3A). Unexpectedly, downregulation of Gal1 expression in PANC-1LUC cells had no effect on tumor size or progression (Supplementary Figure S3B) or on mice survival (Supplementary Figure S3C). Accordingly, no differences in proliferation (Ki67), angiogenesis (von Willebrand factor) or activated stroma (α-SMA) were found between tumors derived from control cells or from shGal1 cells (Supplementary Figure S3D). Importantly, immunohistological analysis showed that, as expected, Gal1 was downregulated in PDA cells from PANC-1LUC shGal1 tumors in comparison to cells from PANC-1LUC shCtl or wt tumors. However, high levels of Gal1 were detected in stromal cells – recruited from the host– present in these shGal1 tumors (Supplementary Figure S3E, arrows). These data, together with those found in *Ela-myc* mice, strongly suggest that Gal1 contribution to *in vivo* tumorigenesis is most likely mediated by the tumor microenvironment, probably through activated fibroblasts and/or immune cells.

Gal1 downregulation affects genes involved in tumor progression, adhesion and migration

From the microarray list obtained after comparing PANC-1 cells with normal or reduced Gal1 levels, we next selected for RT-qPCR validation several genes reported involved in pathways relevant to malignant transformation, some of them previously known to be regulated by Gal1[1] (Supplementary Figure S4). Gal1 was included in the gene validation list as a positive control. Knocked down for Gal1 (shGal1) showed a downregulation of TGFBR3 and FGFR2,

whereas ECM/cell adhesion molecules fibronectin-1, integrin subunit α_5, thrombospondin-1 and E-cadherin were upregulated. These data are in agreement with Gal1 role in tumor cell proliferation[2] and migration/invasion.[3, 4]

Supplementary Figures

Supplementary Figure S1

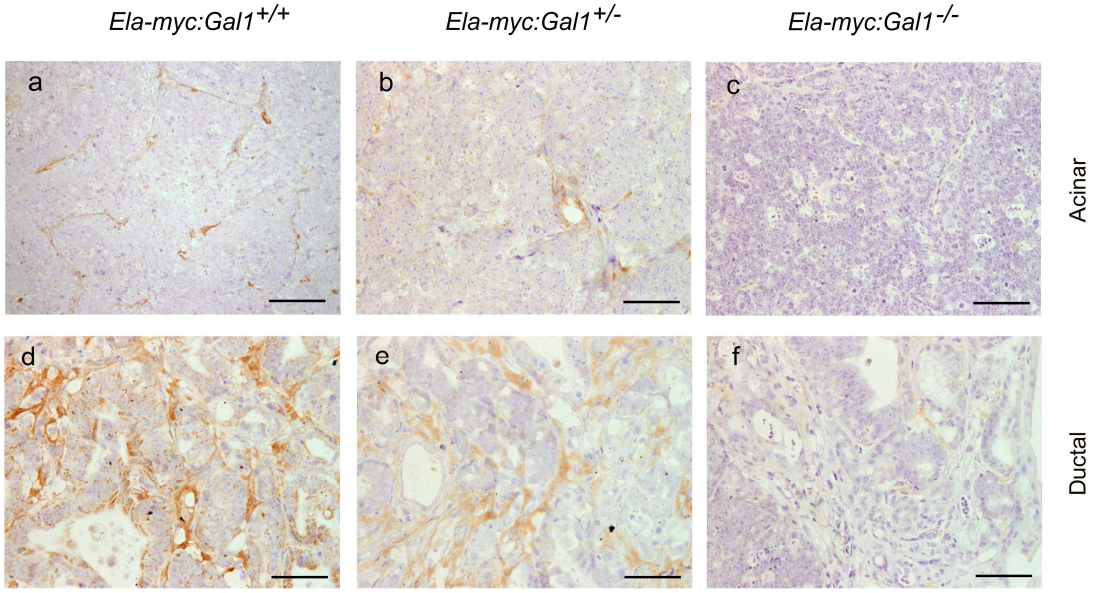

Supplementary Figure S1. Gal1 expression in *Ela-myc:Gal1* tumors. Gal1 immunostaining of acinar (a-c) and ductal regions (d-f) of tumors from *Ela-myc:Gal1*$^{+/+}$, *Ela-myc:Gal1*$^{+/–}$ and *Ela-myc:Gal1*$^{–/–}$ transgenic mice. Bars, 100 µm.

Supplementary Figure S2

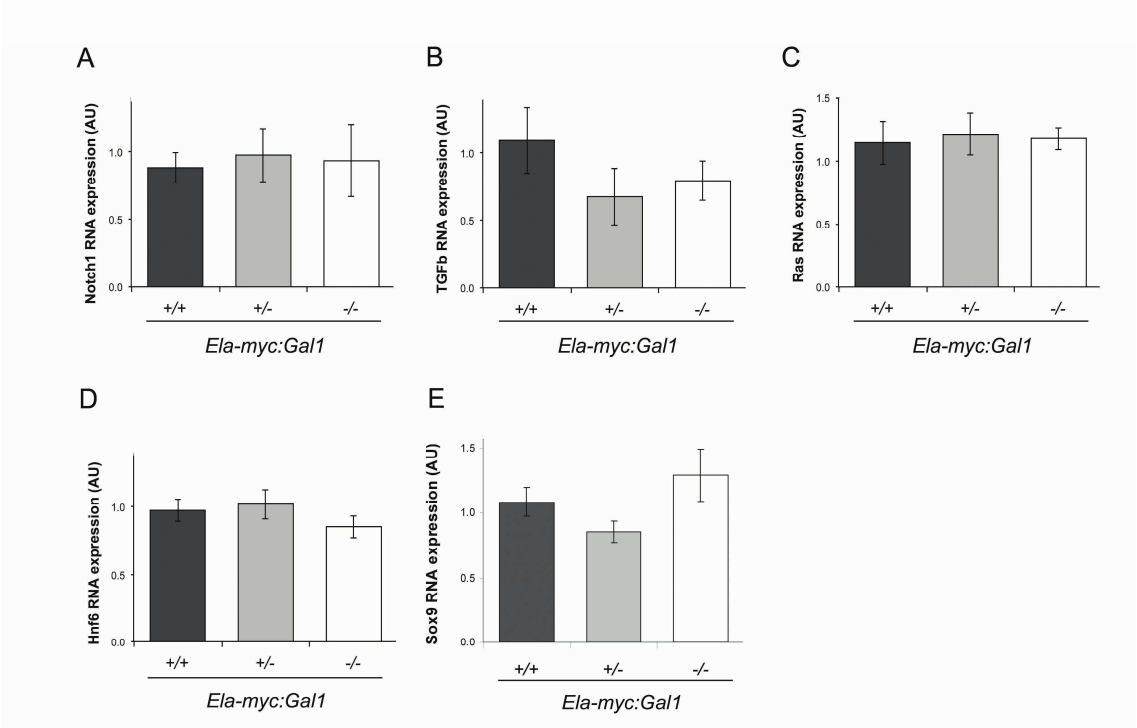

Supplementary Figure S2. RT-qPCR analysis of genes previously involved in acinar-ductal metaplasia but not altered in *Ela-myc:Gal1* tumors. Analysis of genes known to be involved in acinar-ductal metaplasia but not altered by RT-qPCR in extracts from *Ela-myc:Gal1*$^{+/+}$, *Ela-myc:Gal1*$^{+/-}$ and *Ela-myc:Gal1*$^{-/-}$ transgenic mice. All data are mean ± SEM. *P* values (determined by Student's t-test) are relative to *Ela-myc:Gal1*$^{+/+}$ and for all of them $P > .05$

Supplementary Figure S3

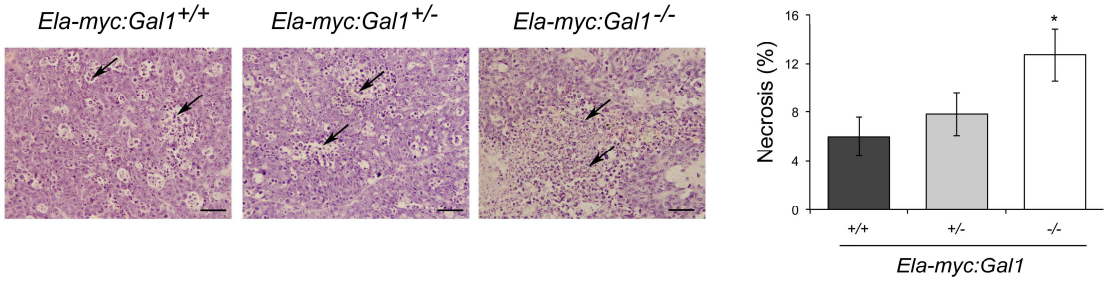

Supplementary Figure S3. Effects of Gal1 depletion in tumor necrosis in *Ela-myc* mice. H&E staining of *Ela-myc* acinar tumors from different Gal1 genotypes showing necrotic areas (arrows). Quantification of the percentage of necrosis is shown on the right. Data are mean ± SEM. *P* values (determined by Mann Whitney test) are relative to shCtl. **P* < .05.

Supplementary Figure S4

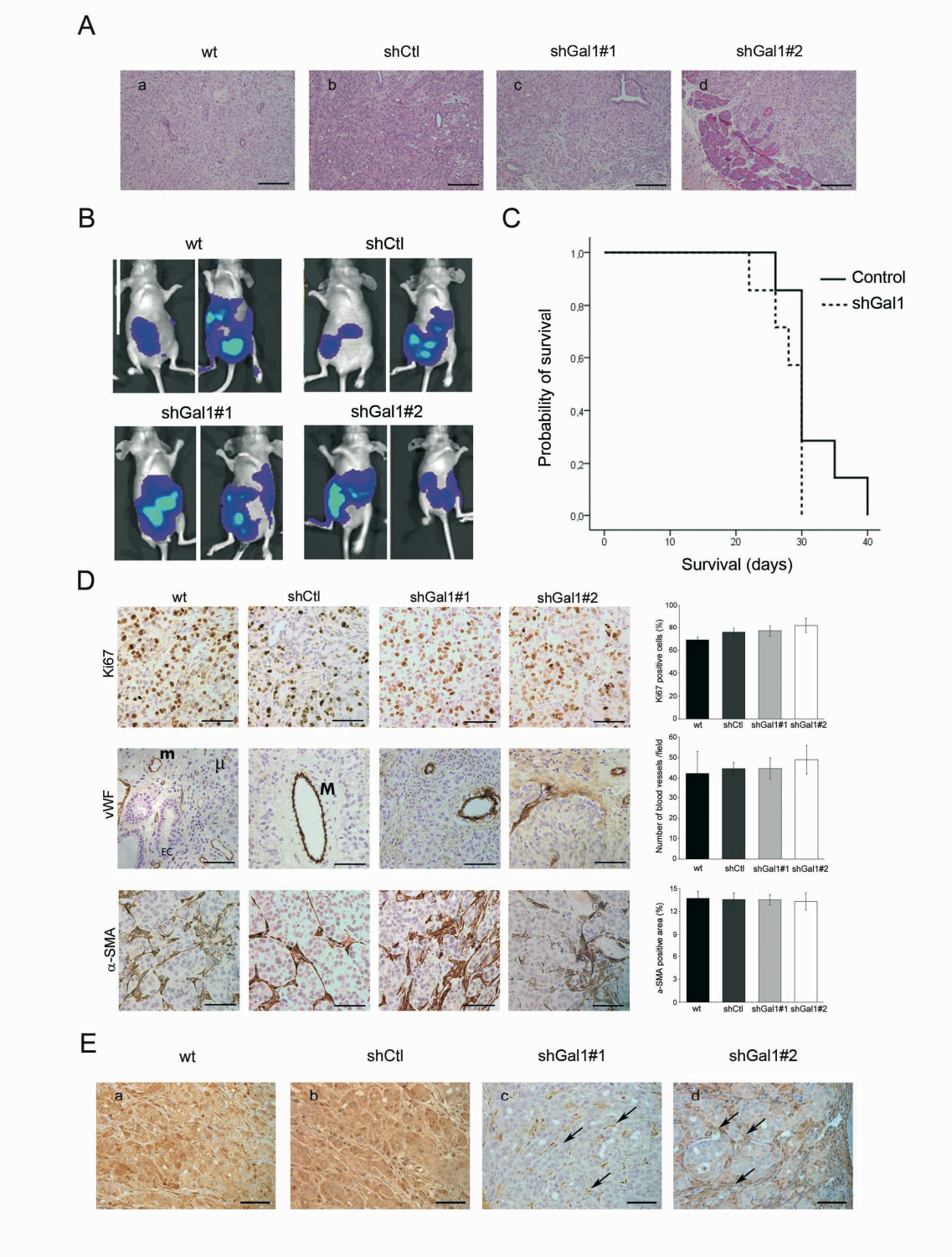

Supplementary Figure S4. Effects of Gal1 downregulation in PDA cells *in vivo*. A. H&E of tissue sections after intraperitoneal injection of non-infected PANC-1 cells (wt), cells infected with an irrelevant shRNA (shCtl) or cells

infected with Gal1 shRNA (shGal1#1 and shGal1#2). Bars, 200 μm. B**.** Two representative mice from each group after 3 weeks of injection are shown. C. Kaplan-Meier survival analysis in tumor-bearing nude mice injected with knockdown Gal1 (shGal1) PANC-1LUC cells (shGal1#1 and shGal1#2; n=7) in comparison to the control group (injected with untransfected or shCtl PANC-1LUC cells (n=7)). *P* values (log-rank test) are relative to control group mice. D. Immunostaining to detect proliferation (Ki67), angiogenesis (vWF) and activated stroma (α-SMA) in tumors from mice injected with untransfected (wt), shCtl or shGal1#1 and shGal1#2 PANC-1 LUC cells. Bars, 100 μm. Bar graphs on the right (A-C), show quantifications, which are represented as the mean positively stained area ± SEM. *P* values (Student's t-test) relative to shCtl were calculated (*P* > .05). E. IHC analysis of Gal-1 in xenograft tumors. Epithelial tumoral cells express high Gal1 levels in wt and shCtl tumors (a, b), whereas undetectable levels were found in shGal1#1 and shGal1#2 tumors (c, d). In contrast, stromal fibroblast, which are derived from the host mice, were strongly positive for Gal1 expression in all tumors, including those from cells with Gal1 downregulation (c, d, arrows). Bars, 100 μm.

Supplementary Figure S5

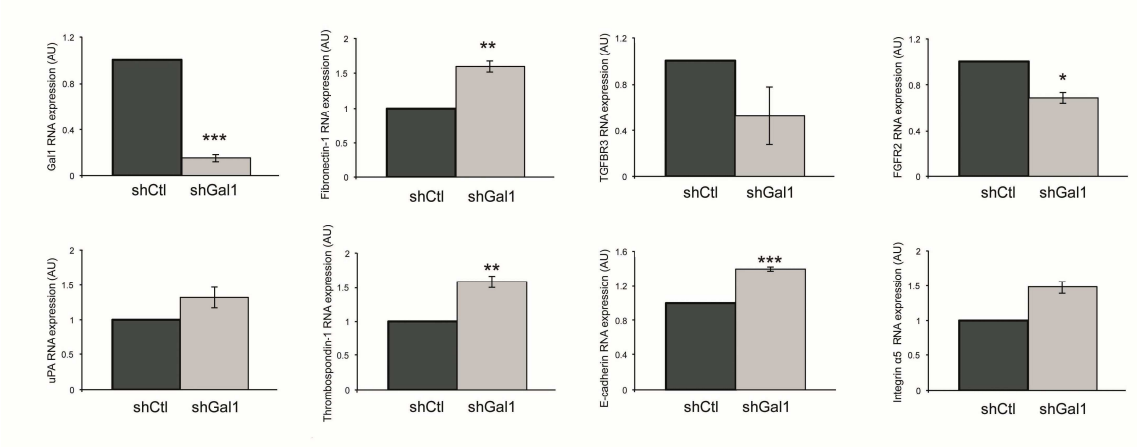

Supplementary Figure S5. Gal1 downregulation affects genes involved in tumor progression, adhesion and migration. Validation by RT-qPCR of mRNAs altered by Gal1 downregulation in PANC-1 cells transfected with an shRNA control (shCtl) or targeting Gal1 (shGal1). *P* values (determined by Student's t-test) are relative to shCtl. **P* < .05; ***P* < .01, ****P* < .001. Gal1 was included as a positive control. Gal1 downregulation (shGal1) correlates with downregulation of TGFBR3 and FGFR2, and upregulation of fibronectin-1, integrin subunit α_5, thrombospondin-1 and E-cadherin.

Legends for Supplementary Videos

Supplementary video 1 (Related to Figure 4D). Time lapse video microscopy in PANC-1 control cells infected with shCtl. Frames were collected every 15 min.

Supplementary video 2 (Related to Figure 4D). Time lapse video microscopy in PANC-1 Gal1 downregulated cells infected with shGal1. Frames were collected every 15 min.

Supplementary Tables

Supplementary Table 1. Tumor invasion and intraperitoneal hemorrhage in *Ela-myc:Gal1*$^{+/+}$, *Ela-myc:Gal1*$^{+/-}$ and *Ela-myc:Gal1*$^{-/-}$ pancreatic tumors.

GENOTYPE	INVASION				INTRAPERITONEAL HEMORRHAGE	
	Lymph nodes		Other organs*			
	Number*	*P* value†	Number¥	*P* value†	Number¥	*P* value†
Ela-myc:Gal1$^{+/+}$	14/44		6/44		14/37	
Ela-myc:Gal1$^{+/-}$	15/55	0.71	11/55	0.48	6/46	0.037
Ela-myc:Gal1$^{-/-}$	12/43	0.77	9/43	0.45	4/42	0.035

* Number of tumor infiltrates or metastasis to lymph nodes or other organs (diaphragm, kidney, liver, intestine, stomach and spleen) respect to the number of total tumors analyzed. ¥ Number of mice with intraperitoneal hemorrhage respect to the number of total mice analyzed for each genotype. † *P* value was determined using Chi-squared method.

Supplementary Table 2. Gene expression profile by microarray analysis of PANC-1 cells with endogenous or downregulated Gal1 levels.

List of genes differentially expressed between shGal1 and shCtl in untransfected PANC-1 cells (wt) and cells transfected with a shCtl or with shGal1 selected by $P < .0005$. This table is available online.

Supplementary Table 3. List of forward and reverse primers used for RT-qPCR.

Gene	*Forward Primer (5'-3')*	*Reverse Primer (5'-3')*
Cyclin-D2	ATT ACC TGG ACC TGG TCT TGG	GCT GGT CTC TTT GAG TTT GGA
Disp-1	ACT CTT CTG ACG GCG TGA CTA	ATG GCT ATG GCA GGA TAC ACA
E-cadherin	CAG TTG AGG ATC CAA TGG AGA	TCT GTC ATG GAA GGT GCT CTT
EGFR	GTG AGC AGA GGC AGG GAG	ATT CTG GAT GGC ACT GGA TG
FGFR2	TGA TGC CAC AGA GAA AGA CCT	GTG CAG GCT CCA AGA AGA TTT
Fibronectin-1	CTG CAG GTC CAG ATC AAA CA	TGA CTC TCT CCG CTT GGA TT
Gal1	CAG CAA CCT GAA TCT CAA ACC	AAA GAC AGC AAC AAC CTG TGC
Hnf6	CCC TGG AGC AAA CTC AAG TC	TTC CCG TGT TCT TGC TCT TT
HPRT	GGC CAG ACT TTG TTG GAT TTG	TGC GCT CAT CTT AGG CTT TGT
Integrin α5	CGT ATC TGC GGG ATG AAT CT	GGG TTG CAA GCC TGT TGT AT
K-Ras	TGC AAT GAG GGA CCA GTA CA	CCA GGA CCA TAG GCA CAT CT
MMP7	TAG GCG GAG ATG CTC ACT TT	GAG AGT GGC CAA ATT CAT GG
Notch1	CCA GGT TTT GCT GGA CAG	GCA GCG GCA ATT GTA GGT AT
Pdx1	TGG ATG AAA TCC ACC AAA GC	TGT AGG CAG TAC GGG TCC TC
Sox9	GGA GGC TGC TGA ACG AGA	CGG GGC TGG TAC TTG TAA TC
TGFb	GCA ACA ACG CCA TCT ATG AG	GGA CAG CAA TGG GGG TTC
TGFBR3	TCA AGC CTG TCT TCA ACA CCT	GGC ACA CAC TTA GGC AAC TTC
Thrombospondin-1	AGA TGG CCA CCA GAA CAA TC	GTC ATC ATC GTG GTC ACA GG
uPA	GTT TGG CAC AAG CTG TGA GAT	GGG AAA TCA GCT TCA CAA CAG

Supplementary Materials and Methods

Animals

All animal procedures were approved by the PRBB Ethical Committee for Animal Experimentation. Transgenic mice were housed as previously described[5, 6] and maintained in groups of four in ventilated cages with 12 h stable light cycles, with a temperature of 22 ± 2 ºC and controlled moisture between 40-70%. Animals were fed *ad libitum* with complete feed. Immunodeficient female BALB/c mice were obtained from Charles River. Founder pairs of *Ela-myc* (C57BL/6 genetic background) were kindly provided by E. Sandgren (University of Wisconsin-Madison, Madison, WI). Male hetereozygous transgenic mice were mated to WT C57BL/6 females to maintain the *Ela-myc* colony. Gal1 knockout mice (C57BL/6 genetic background) came from F. Poirier (Institute Jacques Monod, CNRS, Paris, France). To generate the *Ela-myc:Gal1*$^{+/+}$, *Ela-myc:Gal1*$^{+/-}$ and *Ela-myc:Gal1*$^{-/-}$ mice, mice were crossed in the following manner: for the F1 generation, *Ela-myc* male mice were crossbred with female Gal1$^{-/-}$ to obtain *Ela-myc* heterozygous for Gal1 (*Ela-myc*$^{+/-}$*:Gal1*$^{+/-}$, which represented 50% of the progeny). For the F2, *Ela-myc*$^{+/-}$*:Gal1*$^{+/-}$ males from F1 were paired with Gal1$^{+/-}$ female mice to obtain all genotypes. Littermates were assessed for c-*myc* and Gal1 presence after weaning by DNA tail extraction and PCR analysis. For genotyping, the following primers were used: c-*myc* (5'-CAC CGC CTA CAT CCT GTC CAT TCA AGC-3' and 5'-TTA GGA CAA GGC TGG TGG GCA CTG-3'), expecting a 200 bp band, Gal1 (5'-CTC AGT GGC TAC ATC TGT AAA ATG G-3' and 5'-TTC TTT GAC ATT TGA ACC CTA TACC-3' (3'neo) or 5'-TTC TTT GAC ATT TGA ACC CTA

TACC-3' (3'Gal), expecting a 478 bp band for the wt allele or a 694 bp band for the targeted one.

For xenograft experiments, BALB/c nude mice were injected subcutaneously in both posterior flanks or intraperitoneally with PANC-1LUC control or lentiviral infected cells (2 million cells/ injection). Tumor progression was followed weekly. 100 µL of D-Luciferine (Xenogen) was injected intraperitoneally (16 mg luciferine/Kg). Image was taken after 12 min. Animals were anesthetized with isofluorane and bioluminescence measured for 5 min with IVIS 50 Imaging System (Xenogen). Animal recovery after anesthesia was carefully controlled. In order to localize secondary sites different from the pancreas, luciferase was injected just before animal sacrifice and organ luminescence images were taken afterwards.

Overall survival was calculated from the day of birth to spontaneous death or day of sacrifice determined by tumor size and ethical guidelines, taking into account animal weight loss, antalgic positions, weakness, reduced activity, ascites, jaundice or a palpable abdominal mass. Animals were sacrificed through cervical dislocation. Tumors were weighted and measured through the largest 3 perpendicular diameters to estimate their volume. Major macroscopic features were annotated (shape, vascularization, consistence, color, localization). General aspects were also registered such as splenomegaly, intraperitoneal hemorrages, tumor attachment to intestine or other organs, collapsed intestines, etc. For histology, tumors were fixed in buffered formalin for 24 h, dehydrated and embedded in paraffin. Alternatively, tissue was also harvested in plastic molds (Tissue-Tek Cryomold, Sakura) with OCT embedding medium (Tissue-Tek, OCT Compound, Sakura) and directly frozen in 2-

methylbutane at -80ºC. A sample for RNA preservation was also collected in RNAlater (Sigma).

Histopathology and Immunohistochemistry

For histopathological analysis, tumor sections from *Ela-myc:Gal1*$^{+/+}$ (n=44), *Ela-myc:Gal1*$^{+/-}$ (n=55) and *Ela-myc:Gal1*$^{-/-}$ (n=43) mice, were contrasted with hematoxylin and eosin staining and analyzed by Dr. Jessica Munné and Dr. Mar Iglesias (Pathology Department, Hospital del Mar, Barcelona, Spain). Different parameters were evaluated for each tumor such as the differentiation type (percentage of acinar and ductal components), node infiltration, necrosis, apoptosis and hemorrhage.

For IHC, formalin-fixed paraffin-embedded tissue blocks were sectioned at 5 µm. Sections were deparaffined and antigen retrieval was performed with citrate buffer 0.01 M pH 6.0 at 120ºC for 10 min in a pressure cooker (all antibodies) or with pepsin 0.1% in HCl 0.1 M, 20 min 37ºC (only for von Willebrand Factor (vWF)). Endogenous peroxidase activity was quenched with H_2O_2 3% for 10 min and blocking was achieved with PBS 1% BSA. Primary antibodies were added overnight at 4ºC. Antibodies used for specific tissue immunostaining included α-Gal1 (kindly provided by Dr. Gabius, Ludwig-Maximilians-University, Munich, Germany), α-Ki67 (Novo Castra), α-SMA, (Sigma), α-vWF (Neomarkers), α-CD3e (Santa Cruz) and α-MPO (Dako). Non-immune (Sigma) or pre-immune rabbit serum were used as negative controls. As secondary antibodies, peroxidase-conjugated (Envision+) anti-rabbit and anti-mouse Ig reagents from Dako were used for 1h, RT. Reactions were developed using 3,3'-diaminobenzidine (DAB) as chromogenic substrate. Sections were

counterstained with hematoxylin, dehydrated, and mounted. For visualization, an Olympus BX61 microscope was used and images were acquired using CellSens software.

For immunohistochemistry quantification, 15 animals per group were taken, analyzing 10 images at 10X for each of them by means of ImageJ software. For proliferation, the percentage of Ki67 positive cells in ductal regions was obtained by relating the area corresponding of Ki67 positive nuclei and the total nuclei area (positive for hematoxylin). To quantify angiogenesis and stromal abundance, the area corresponding to vWF or α-SMA positive staining, respectively, was related to total area. In these cases, both acinar and ductal tumoral regions were analyzed. To obtain the global value, data was gathered considering the percentage of acinar versus ductal areas and its angiogenic or stromal score. For T lymphocyte and neutrophil quantification, 10 tumors per group were stained with CD3 or MPO, respectively, analyzing 10 images at 10X per animal with ImageJ software.

Cell lines and *in vitro* functional experiments

All cells were cultured in DMEM supplemented with 10% FBS at 5% CO_2 and 37ºC. Pancreatic tumoral cells PANC-1[8] and RWP-1[7] cells were used for Gal1 downregulation and overexpression, respectively. HEK-293T cells[8] were used for lentivirus generation. F88.2 cells were spontaneously immortalized fibroblasts from a breast tumor (a kind gift from F.X. Real, CNIO, Spain). HPSE were generated as previously described.[9]

For migration studies, wound healing experiments were performed. Briefly, cells were seeded over sterile coverslips and left in DMEM with 10% FBS until tight

confluence. A wound was performed by detaching cells with a micropipette tip and cells were left in DMEM 0.5% FBS to follow migration. Wound closure was quantified using ImageJ software analysis.

For mobility experiments, time-lapse video microscopy was used. Cells were seeded 24 h before the mobility assay in borosilicate coverglass 4 chamber plates (LabTek). Pictures were taken every 15 min for 10 h (5 fields/cell line) with a Zeiss Cell Observer HS microscope. Recorded trajectories were analyzed and the greatest linear distance was measured and quantified using Manual Tracking software for ImageJ. 25 cell trajectories per cell line were monitored.

For proliferation, 50000 cells were seeded over T24 sterile coverslips. BrdU at 40 μM was incubated for 10 min in cells seeded over coverslips. Cells were fixed in 4% PFA and treated for 10 min with HCl 4 M. Permeabilization was achieved with 0.2% Triton in PBS and blocking with 5% BSA, 0.1% Tween20. Coverslips were incubated with a mouse α-BrdU (Santa Cruz Biotechnologies), α-mouse Alexa Fluor 488 (Invitrogen) and DAPI (0.25 μg/mL) for nuclei visualization. Coverslips were mounted with Fluoromont-G and IF detected with an Olympus BX61 Microscope. 10 fields per coverslip were used for quantification. The number of BrdU positive cells were manually counted and compared to total number of cells (DAPI positive) for each experiment. Quantification data were normalized to 1 in order to be able to compare between experiments.

For anchorage independent growth, cells were seeded in DMEM 0.3% Noble Agar over a compacter layer of DMEM 0.7% Noble Agar. DMEM 10% FBS was

added on the top, supplementing every 72 h. Colony number was counted after 6 weeks, helping visualization with MTT staining (1 mg/mL, 4 h, 37ºC).

Gal1 knockdown by shRNA or siRNA

For lentiviral infection of PANC-1 Cells, HEK-293T cells were transfected using PEI with three lentiviral packing vectors (pRSV-rev, pHCMV-G, pMDLg/pRRE) and the vector containing Gal1 shRNA (pLKO-1-puro vector, MissionRNAi, TRCN0000057423-427) or a non-targeting shRNA (shCtl, Sigma (SHC002)). Their supernatant was collected at 48 and 72 h, filtered (0.45 μm) and polybrene was added (8 μg/mL). PANC-1 or PANC-1LUC cells were subsequently infected by adding polybrene to supernatants and selected with puromycin at 3 μg/mL.

Microarray Analysis

RNA extraction from cell lysates was performed with RNeasy Plus Mini kit (Qiagen), having been previously purified with Qiashredder columns (Qiagen). Purity and integrity of the RNA were assessed by spectrophotometry and nanoelectrophoresis using the NanoDrop ND-1000 spectrophotometer (NanoDrop Technologies) and the Nano lab-on-a-chip assay for total eukaryotic RNA using Bioanalyzer 2100 (Agilent Technologies), respectively. Microarray expression profiles were obtained using the Affymetrix Human Exon ST 1.0 arrays (Affymetrix) in IMIM's Microarray facility (Barcelona). Briefly, 1 μg of total RNA from each sample was processed, labeled and hybridized to Affymetrix Human Exon ST 1.0 arrays according to the Affymetrix GeneChip Whole Transcript Sense Target Labeling Assay described below. After quality control of raw data, it was background corrected, quantile-normalized and summarized

to a gene-level using the robust multi-chip average (RMA)[12] obtaining a total of 18708 transcript clusters, which roughly correspond to genes. Normalized data were then filtered to avoid noise created by non-expressed transcript clusters in the condition. Only transcripts over 75% of variance from total variance were considered for further analysis, which led to 4612 transcript clusters. Core annotations (version netaffx 32, human genome 19) were used to summarize data into transcript clusters. Linear Models for Microarray (LIMMA),[10] a moderated t-statistics model, was used for detecting differentially expressed genes between PANC-1 shGal-1 and PANC-1 cells infected with a control shRNA (shCtl). Only genes with a *P* value less than .0005 were selected as significant. Functional analysis was performed using Hypergeometric-based tests against the Biological Process GO ontology with genes selected as having a multiple comparison false discovery rate P-value smaller than 0.0005. Hierarchical cluster analysis was also performed to see how data aggregated. All data analyses were performed in R (version 2.15.0) with packages aroma.affymetrix, Biobase, Affy, limma, genefilter, Category and GOstats.[10, 11]

For validation by qRT-PCR, total RNA was extracted from cultured cells with the RNeasy kit (Qiagen) and first strand cDNA was prepared from RNA using random hexamer primers and the RevertAid first strand cDNA synthesis kit (Fermentas). HPRT was used to normalize cDNA inputs. qRT-PCR primers were designed with Oligo Perfect Designer (Invitrogen) (Supplementary Table 3). For the human PANC-1 cell line validation: 10 µL sample reactions for RT-qPCR were prepared with SybrGreen Master Mix (Applied Bioscience) and 25 ng of sample. RT-qPCR was performed in ABI7900HT (Applied Biosystems).

Supplementary References

1. Camby I, Decaestecker C, Lefranc F, et al. Galectin-1 knocking down in human U87 glioblastoma cells alters their gene expression pattern. Biochem Biophys Res Commun 2005;335:27-35.

2. Kopitz J, von RC, Andre S, et al. Negative regulation of neuroblastoma cell growth by carbohydrate-dependent surface binding of galectin-1 and functional divergence from galectin-3. J Biol Chem 2001;276:35917-35923.

3. Camby I, Belot N, Rorive S, et al. Galectins are differentially expressed in supratentorial pilocytic astrocytomas, astrocytomas, anaplastic astrocytomas and glioblastomas, and significantly modulate tumor astrocyte migration. Brain Pathol 2001;11:12-26.

4. van den Brule FA, Buicu C, Baldet M, et al. Galectin-1 modulates human melanoma cell adhesion to laminin. Biochem Biophys Res Commun 1995;209:760-767.

5. Poirier F, Robertson EJ. Normal development of mice carrying a null mutation in the gene encoding the L14 S-type lectin. Development 1993;119:1229-1236.

6. Sandgren EP, Quaife CJ, Paulovich AG, et al. Pancreatic tumor pathogenesis reflects the causative genetic lesion. Proc Natl Acad Sci U S A 1991;88:93-97.

7. Dexter DL, Matook GM, Meitner PA, et al. Establishment and characterization of two human pancreatic cancer cell lines tumorigenic in athymic mice. Cancer Res 1982;42:2705-2714.
8. Pear WS, Nolan GP, Scott ML, et al. Production of high-titer helper-free retroviruses by transient transfection. Proc Natl Acad Sci U S A 1993;90:8392-8396.
9. Hwang RF, Moore TT, Hattersley MM, et al. Inhibition of the hedgehog pathway targets the tumor-associated stroma in pancreatic cancer. Mol Cancer Res 2012;10:1147-1157.
10. Smyth GK. Linear models and empirical bayes methods for assessing differential expression in microarray experiments. Stat Appl Genet Mol Biol 2004;3:Article3.
11. Irizarry RA, Hobbs B, Collin F, et al. Exploration, normalization, and summaries of high density oligonucleotide array probe level data. Biostatistics 2003;4:249-264.